PREDICTION OF IMMUNE CHECKPOINT INHIBITOR THERAPY IN UROTHELIAL CARCINOMA: INTEGRATED ANALYSIS OF MOLECULAR PATTERNS AND CLINICAL FACTORS

PhD thesis

Melinda Rita Hermann-Váradi

Semmelweis University Doctoral School

Surgical Medicine Division

Supervisor: Tibor Szarvas, D.Sc.

Official reviewers: Csaba Bödör, D.Sc.

Tamás Beöthe, MD, Ph.D.

Head of the Complex Examination Committee:

Ilona Kovalszky, MD, D.Sc.

Members of the Complex Examination Committee:

Gábor Lotz, MD, D.Sc.
Tibor Füle, Ph.D.

Budapest
2025

1. Introduction

Urothelial carcinoma (UC) is the second most common urological cancer, that can develop in both the lower (bladder and urethra) and the upper urinary tract (renal pelvis and ureter). Bladder cancer (BC) accounts for 90–95% of UCs whilst upper tract urothelial carcinomas (UTUC) account for only the remaining 5–10%. BC presents a major challenge to global healthcare systems, ranking as the ninth most common cancer worldwide. More than 90% of BCs are urothelial (transitional cell) carcinomas. Based on histological staging, BC can be classified into non-muscle-invasive (NMIBC) and muscle-invasive (MIBC) forms. About 70% of newly diagnosed cases are NMIBC, while in approximately 30% of patients, the tumor has already invaded the muscularis propria of the bladder wall. All MIBC cases are poorly differentiated, also referred to as high-grade UCs. MIBC patients often face high rates of disease recurrence, progression, and mortality, even after undergoing comprehensive treatments such as radical surgery (cystectomy) and neoadjuvant or adjuvant therapies. Approximately 40% of these patients experience metastatic relapse, while 5% are initially diagnosed with metastatic disease. The 5-year overall survival (OS) rate for metastatic UC (mUC) is around 9%.

For decades, platinum-based chemotherapy has been the standard first-line systematic treatment for MIBC. Recent randomized controlled trials and real-life studies have challenged the dominance of cisplatin-based chemotherapy, exploring the benefits of other systematic therapies such as immune checkpoint inhibitors (ICIs), the FGFR-inhibitor erdafitinib, and the antibody-drug conjugates. Although ICIs have shown impressive efficacy in a subset of UC patients, challenges such as drug resistance and side effects persist. About only 20–30% of mUC patients benefit from the ICI therapy, and fewer patients could experience durable responses lasting more than 2 years. These facts highlight the growing need for reliable biomarkers to guide treatment selection and better predict which patients are most likely to benefit from ICI therapy. As the therapeutic landscape for mUC continues to evolve, the development of robust and clinically relevant biomarkers remains crucial for refining patient selection and optimizing treatment outcomes

2. Objectives

The aim of the study is to gain a better understanding of the factors affecting the effectiveness of ICI therapy under real-world conditions and to identify new potential predictive molecular markers or set of markers. The work presented here has two main parts: clinical data analysis and molecular analyses (Figure 1).

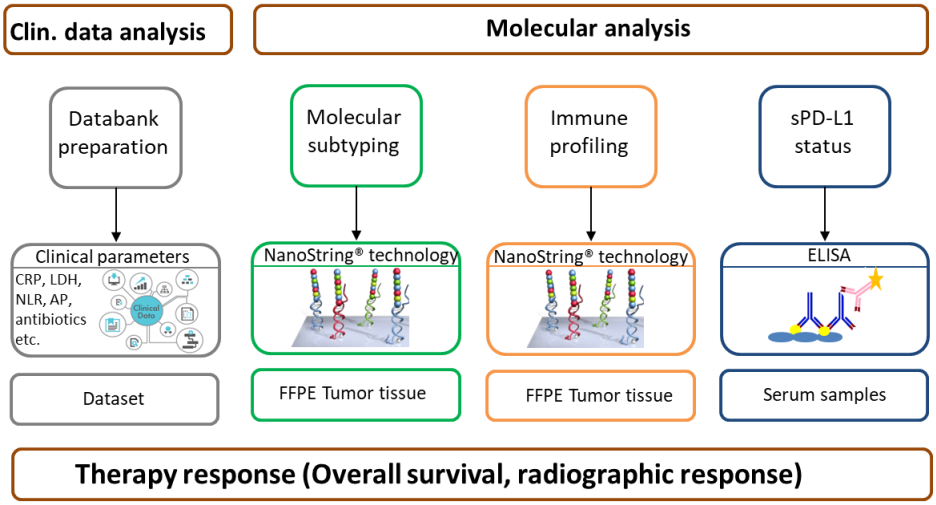

Figure 1. Overview of the research plan (Own figure)

2.1. Aims of the retrospective clinical data analysis

This multicentric, retrospective study aimed:

1. To assess the characteristics of UC patients receiving ICI treatment in routine clinical settings.
2. To compare the effectiveness of two widely used ICI drugs (pembrolizumab and atezolizumab) against results from respective clinical trials.
3. To evaluate the prognostic significance of standard clinicopathological and laboratory parameters.

2.2. Aims of the molecular analyses

1. To identify potential ICI-predictive genes in our institutional UC patient cohort through gene expression analysis of the tumor and its microenvironment.
2. To develop a prognostic model by combining clinicopathological and molecular factors.
3. To examine how different molecular subtypes of UC relate to therapy response and survival outcomes in patients undergoing ICI treatment
4. To evaluate the prognostic value of soluble PD-L1 (sPD-L1) as a serum biomarker

3. Methods

3.1. Clinical data analysis

Eligible patients included adults (≥18 years) with a confirmed diagnosis of advanced or metastatic urothelial tract malignancy who received at least one cycle of ICI (pembrolizumab or atezolizumab) as first-, second-, or later-line treatment between January 2017 and December 2021. Patient data were obtained from medical records and respective files across 6 uro-oncology centers, collecting clinicopathological, laboratory and clinical outcome data. The end date for data analysis was August 2022. The study conformed to the Declaration of Helsinki, and the regional ethics committee approved the protocol (approval no.: SE RKEB 125/2019).

Overall survival (OS) was used as the primary endpoint of this study because it is a robust and objective endpoint; moreover, information on response and progression was not always available. Secondary outcomes included progression-free survival (PFS), objective response rate (ORR), disease control rate (DCR), and duration of response (DOR). Treatment response was determined by the data collector based on radiographic studies and clinical notes. ORR was defined as the percentage of patients achieving a partial or complete response (PR or CR) to treatment within the follow-up period, while DCR referred to the proportion of patients with CR, PR, or stable disease (SD).

Descriptive statistics included the median and range for continuous variables and counts with percentages for categorical variables. All time-to-event data (OS, PFS, DOR) were visualized using Kaplan-Meier estimates, with medians reported alongside corresponding 95% confidence intervals (CIs). The median and range of time to response were reported for patients with CR and PR. Cox proportional hazards models were used to assess differences in hazard ratios (HRs) between groups according to risk factors, and a stratified two-sided log-rank test was employed to assess differences in OS. A Chi-Squared Test of Independence was conducted to determine associations between response (CR/PR) or disease control (CR/PR/SD) and various clinicopathological variables. A p-value of <0.05 was considered statistically significant. All statistical analyses were performed with IBM SPSS Statistics, version 27.0 (IBM Corp., Armonk, NY, USA).

3.2. Molecular analyses – gene expression analysis

The study included advanced or metastatic UC patients with available formalin-fixed, paraffin-embedded (FFPE) tumor samples, who received at least one cycle of ICI

therapy (pembrolizumab or atezolizumab) as first- or second-line treatment between January 2017 and February 2023. The study conformed to the Declaration of Helsinki, and the respective ethics committees approved the study protocol (SE RKEB 125/2019, 15–6400-BO, 2021–1548).

Samples from radical surgeries (cystectomy or nephroureterectomy) or transurethral bladder resections were prepared for gene expression analysis. RNA was extracted from 10 µm-thick FFPE tissue sections (2–10 slides per case). To reduce contamination with non-malignant tissue, macrodissection was performed, focusing only on marked tumor areas with >50% tumor cell content. Selected areas were carefully scraped, and RNA was isolated using the MagMAX™ FFPE DNA/RNA Ultra Kit (Thermo Fisher Scientific, Waltham, MA, USA) per the manufacturer's protocol. Extracted RNA concentrations were measured with the Qubit™ RNA High-Sensitivity Assay Kit and the Qubit fluorometer (Thermo Fisher Scientific, Waltham, MA, USA). Samples with sufficient RNA concentrations (>30 ng/µL) were hybridized to the NanoString nCounter® PanCancer IO 360™ Gene Expression Panel (NanoString, Seattle, WA, USA) for 24 hours in a thermocycler. Samples were processed on the nCounter Prep Station (NanoString, Seattle, WA, USA), and gene expression profiles were digitized using the nCounter Digital Analyzer.

For molecular subtype classification according to the MDA, Lund, TCGA and consensus classification systems, we used a gene panel based approach with 48 genes covering six tumor cell-specific (luminal, basal, squamous, neuronal, epithelial-to-mesenchymal transition (EMT), and in situ carcinoma [CIS]) as well as three stroma-related gene signatures (p53, extracellular matrix (ECM)/smooth muscle (SM), and immune cell-specific). NanoString nCounter® analysis with a custom gene panel of 48 subtype-specific genes and 19 additional single genes was conducted, as previously described.

The NanoString data analysis was conducted within the R for Windows environment (v4.4.0, R Foundation for Statistical Computing, Vienna, Austria, 2024). Normalized NanoString data was compared using Wilcoxon rank-sum tests. Survival analysis utilized Cox regression models. All p-values were FDR-corrected using the Benjamini- Hochberg method. The Random Survival Forest (RSF) model was used to combine the significant factors identified from the univariate analysis to predict survival

outcomes. To validate the prognostic value of selected genes, the online tool "Kaplan-Meier Plotter" was used to analyze publicly available gene expression and survival data across cancer datasets, including ICI-treated UC cases. Additionally, the "ROC Plotter" tool was employed to assess the diagnostic and predictive performance of differentially expressed genes. Both pan-cancer and UC-specific (IMvigor210) validations were performed.

3.3. Molecular analyses – determination of sPD-L1 levels

Pre-treatment serum samples were collected from 12 UC patients who underwent ICI therapy with either atezolizumab (n = 11) or pembrolizumab (n = 1). The samples were obtained between April 2019 and March 2020 at the Department of Urology, Semmelweis University. On-treatment serum samples, collected before the second immunotherapy cycle, were available for 92% (11/12) of the patients. The study was conducted in accordance with the Helsinki Declaration and approved by the institutional ethics committee (TUKEB 55/2014 and 224/2013). Written informed consent of all patients was available.

Soluble PD-L1 levels in serum samples were measured using the PD-L1/B7-H1 Quantikine ELISA kit (DB7H10, R&D Systems, Wiesbaden, Germany) following the manufacturer's protocol. The ELISA plates were read using the Thermo Scientific™ Multiscan FC Microplate Photometer with SkanIt 5.0 Software. For dichotomization, the cut-off values were defined as the median (90 pg/mL). To rule out potential interference or cross-reactivity between the therapeutic anti-PD-L1 antibody (atezolizumab, Tecentriq®, Roche, Basel, Switzerland) and the ELISA kit, additional ELISA analyses were performed using atezolizumab and pembrolizumab. The low number of cases did not allow a valid statistical analysis.

4. Results

4.1. Clinical data analysis

4.1.1. Patient characteristics

Data from 210 eligible patients were analyzed. Seventy-six patients received atezolizumab, and 134 patients received pembrolizumab. The median age at the start of ICI therapy was 67.3 years (range: 28.9–87.2 years). The most common primary tumor localization was in the bladder, affecting 81.9% of patients. Twelve cases (5.7%) presented with tumors in both locations (upper urinary tract and bladder). Ninety-one patients (43.3%) underwent radical surgery (cystectomy or nephroureterectomy), and 22 patients (10.5%) received radiochemotherapy as local treatment. At the time of ICI initiation, 31.9% of patients had lymph node-only metastases, and 45.2% had visceral metastases. The majority of patients (83.3%) were categorized into ECOG PS groups ≤1.

We had sufficient data for 184 patients to classify them according to the Bellmunt criteria. The Bellmunt risk score classifies patients into risk groups based on three factors: ECOG PS >0, hemoglobin (Hgb) level <10 g/dL, and the presence of liver metastases. The distribution of risk groups was as follows: 35.2% had no risk factors (Bellmunt 0), 38.6% had one risk factor (Bellmunt 1), 11.4% had two risk factors (Bellmunt 2), and 2.4% (5 patients) had three risk factors (Bellmunt 3). In the first-line cohort, more than half of the patients had at least one risk factor.

4.1.2. Real-world efficacy (tumor responses, PFS, OS) of ICIs

Patients received a median of 6 treatment cycles (range: 1–80) and remained on therapy for a median of 4.3 months. At the time of the data cut-off, 31 patients (14.8%) were still receiving ICI therapy. The primary reason for discontinuing treatment was disease progression. The median follow-up period after ICI initiation was 10.2 months. No radiographic response data was available for 29 patients. Among the 181 patients evaluable for radiographic response, 13 achieved a complete response, and 53 had a partial response. The overall response rate (ORR) for the entire cohort was 36.5%, with ORRs of 32.9% in the first-line setting and 38.9% in the second-line setting. The median duration of response (DOR) was 11.8 months. Disease control was achieved in 112 patients, resulting in a disease control rate (DCR) of 61.9% for the entire cohort.

The median PFS was 5.9 months (95% CI: 3.9–7.8 months). For first-line ICI treatment, the median PFS was 7.2 months (95% CI: 4.2–10.3 months), while for second-line treatment, it was nearly 3 months shorter, at 4.4 months (95% CI: 2.3–6.5 months). A total of 140 patients (66.7%) died during the study period. The median OS was 13.6 months (95% CI: 9.4–17.7 months).

4.1.3. Determinants of OS and PFS

In univariate Cox regression analysis, radical surgery, only lymph node metastases, high hemoglobin, albumin, and eGFR levels prior to therapy initiation were significantly associated with improved OS. In contrast, the presence of liver metastases, visceral metastases or bone metastases, impaired ECOG PS, the presence of any Bellmunt risk factor, and elevated NLR values (≥5) were identified as prognostic factors for shorter OS.

In Cox regression analysis examining PFS, age over 68 years at ICI initiation, lymph node metastases, hemoglobin, and albumin levels above the cut-off were associated with improved PFS. On the other hand, the presence of liver metastases, visceral metastases, bone metastases, ECOG PS > 0, NLR ≥5 and Bellmunt risk group 1+ were associated with worse PFS. Univariate Cox regression analyses were also performed separately for the first- and second-line treatment groups, with the results for the second-line subgroup being similar to those for the whole cohort.

The multivariable analysis included all variables that showed a significant association with survival and for which data were available for at least 85% of cases. In multivariate analysis, ECOG PS, the presence of visceral or bone metastases, and hemoglobin levels ≥10 g/dL were identified as independent prognostic factors for OS. The presence of one or more Bellmunt risk factors was found to be an independent prognostic factor for shorter OS and PFS as well.

4.1.4. Determinants of treatment response and disease control

Information on response during ICI therapy was available for a subset of patients (n=181). Among the clinical parameters, age at ICI initiation, ECOG PS, the presence of liver, bone, or LN metastases, and Bellmunt risk factors showed significant associations with response and disease control. Additionally, two laboratory parameters, NLR and albumin level, also showed a significant association with these outcomes.

4.1.5. Comparison of the real-world cohort with corresponding clinical trial cohorts

Although the multicenter design of this study enabled the inclusion of a diverse group of patients reflective of real-world clinical practice, the characteristics of our cohort—such as age, sex, and primary tumor location—were largely comparable to those reported in the corresponding clinical trials (KEYNOTE-045, KEYNOTE-052, IMvigor211, and IMvigor210), with only minor differences. Interestingly, our real-world cohort included a lower rate of liver metastases, an unexpected finding given that investigators often tend to select more fit patients for inclusion in clinical trials.

The ORRs observed in our study were similar to those reported in the clinical trials, with the exception of second-line atezolizumab treatment. In this setting, the ORR of the real-life cohort (34.5%) was more than 20% higher compared to the respective clinical trials (14.5% and 13.3% in IMvigor210/cohort 2 and IMvigor211, respectively).

The median OS time for our entire cohort was 13.6 months. When patients were grouped by the administered drugs and treatment settings, the poorest OS was observed in the first-line atezolizumab-treated subgroup, although the case numbers in this group were low. A notable OS difference was seen in the second-line atezolizumab-treated groups, with the real-life cohort showing a median OS of 17.0 months, compared to 7.9 and 11.1 months reported in IMvigor210/cohort 2 and IMvigor211, respectively.

4.2. Gene expression analysis

4.2.1. Cohort description and follow-up details

The patient cohort included in the gene expression analysis consisted of 100 UC patients. Among patients, 34 received atezolizumab and 66 received pembrolizumab. The median age at therapy initiation was 70.3 years (range: 30.9–88.8 years). Bellmunt risk scores could be calculated for 97% of the patients, and data on PD-L1 IHC positivity were available in 77 cases.

The median follow-up from ICI therapy baseline was 12.0 months. Of the 99 patients with available radiographic responses, three experienced complete remission (CR), and 31 had a partial response (PR), resulting in an ORR of 34%. Disease control was achieved in 58 patients. The median PFS was 4.9 months (95% CI: 3.4–8.6). During the follow-up, 75 patients passed away, and the median OS was 13.6 months (95% CI: 9.1–18.4).

4.2.2. Clinicopathological factors associated with survival or therapy response

As there were significant overlaps between the real-life cohort described previously and the gene expression analysis cohort, the results of the statistical analyses for the gene expression cohort, including Cox regression and Chi-squared tests, were similar to those presented in previous chapters.

4.2.3. Differential gene expression and survival

In total, 95 genes were associated with OS. Of these, 23 genes remained significant after false discovery rate (FDR) correction. Subsequent validation using the KM Plotter online tool in the transcriptome dataset from the IMvigor210 study (second-line atezolizumab in over 300 mUC patients) confirmed the prognostic value of 6 genes.

4.2.4. Differential gene expression and therapy response

The Wilcoxon test identified 20 genes (analyzed as continuous variables) significantly associated with ORR. Genes linked to good ORR included *MAGEA12*, *SPP1*, *GPI*, *ENO2*, *TFRC*, *BST1*, *C3*, *MME*, *MAGEA3*, *PRAME*, *NFKBIA*, and *CTAG1B*, while those associated with poor ORR included *TMEFF2*, *FLT4*, *ABCB1*, *CCL24*, *CREBBP*, *CD209*, *C8G*, and *MYD88*. Furthermore, 43 genes were associated with disease control (DCR). Validation using the ROC Plotter online tool in the pan-cancer dataset revealed 16 differentially expressed genes (Figure 2). Among these, *IRF1* and *PSMB10* also exhibited significantly different expression levels in the validation UC cohort from the transcriptome dataset of IMvigor210. Notably, *PSMB10* was the only gene validated for both endpoints: DCR and OS (Figure 3).

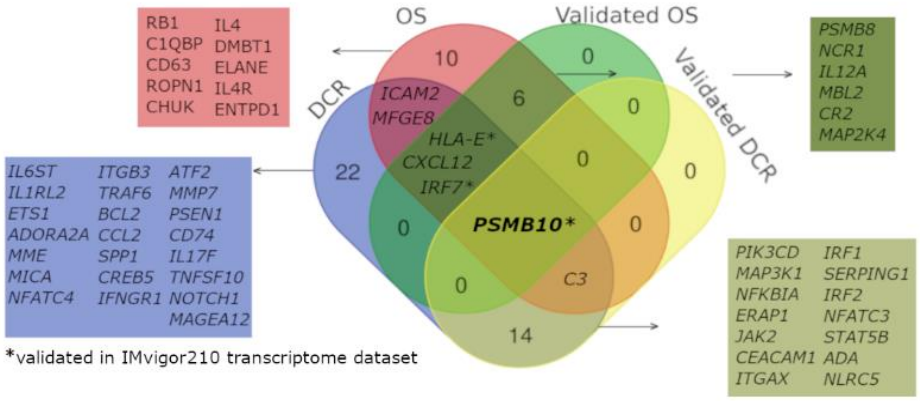

Figure 2. Venn diagram illustrating overlapping associations of genes with different endpoints. (Own figure)

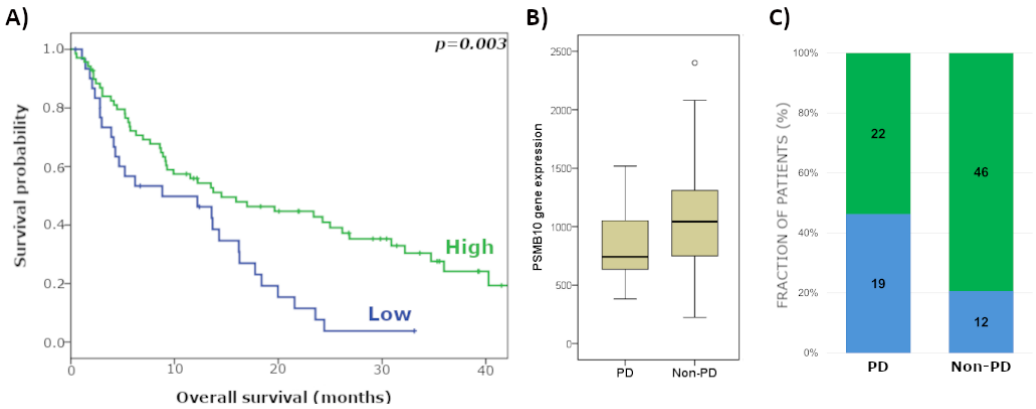

Figure 3. Survival (A) and therapy response (boxplots (B) and bar charts (C)) based on gene expression levels of PSMB10. Blue bars represent low gene expression, and green bars represent high gene expression.(Own figure)

4.2.5. Correlation of molecular subtypes with survival and therapy response

We identified molecular subtypes using four different classification systems (MDA, TCGA, Lund, and consensus). No significant differences were observed in OS or PFS among the consensus and Lund-classification subgroups (p=0.575 for OS and p=0.441 for PFS in both systems) (Figure 4A and C). However, patients in the MDA-p53-like subgroup demonstrated significantly longer OS (p=0.024) and PFS (p=0.043) compared to those in the luminal and basal subgroups (Figure 4D). According to the TCGA classification system, the luminal subgroup showed inferior OS (p=0.023) and PFS (p=0.038) compared to other groups. Additionally, the neuronal and luminal-

infiltrated subtypes exhibited longer OS, though the number of cases in the neuronal group was limited (Figure 4B).

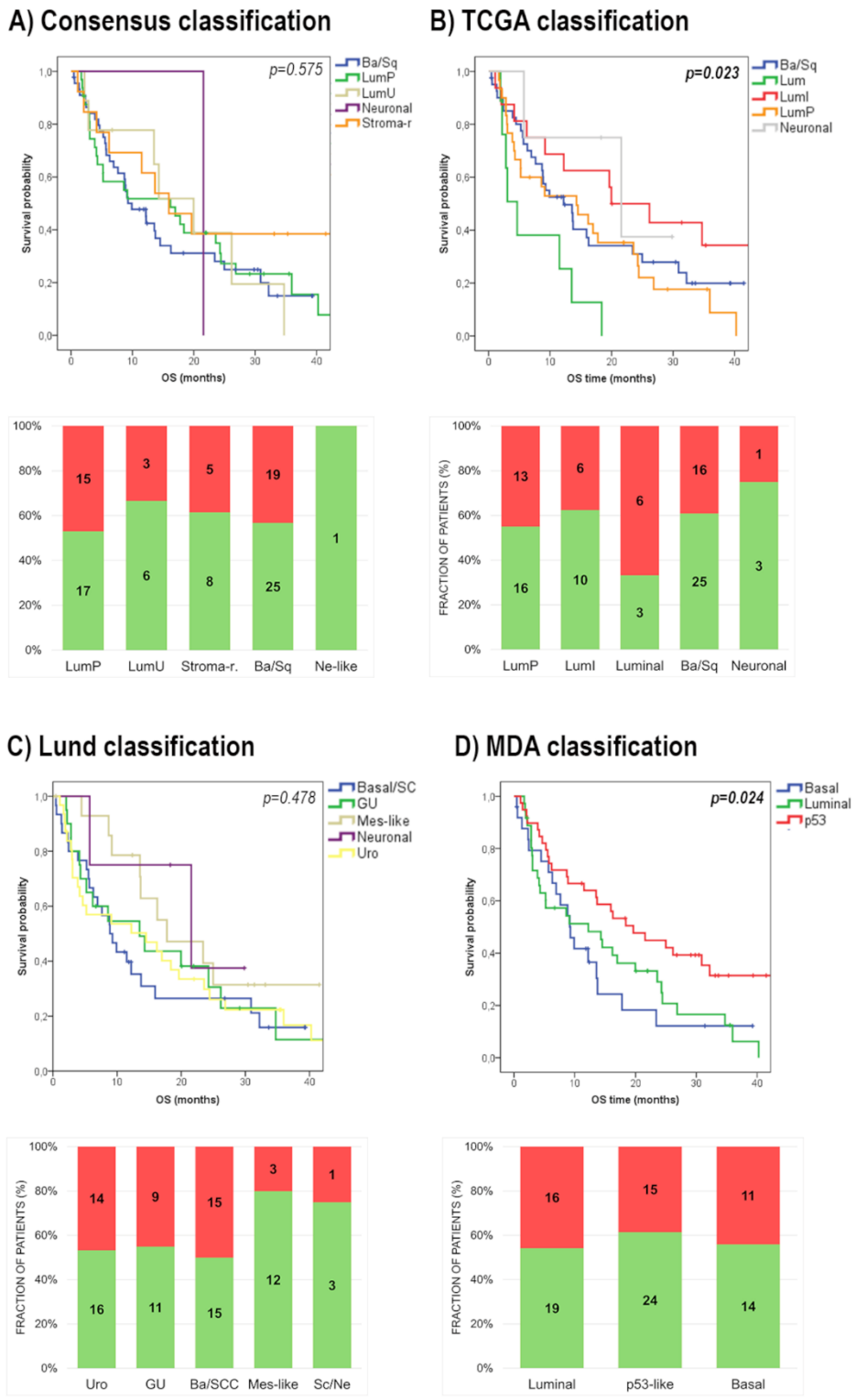

Figure 4. Survival and radiographic response of different molecular subtypes. Radiographic response is indicated as green for non-progressive disease (non-PD) and red for progressive disease (PD). Subtypes are shown based on the (A) consensus, (B) TCGA, (C) Lund, and (D) MDA classification systems. (Own figure)

Among the evaluated signature scores, high neuronal scores (≥3.2), calculated from the expression levels of 10 genes — *APLP1, CHGB, ENO2, GNG4, MSI1, PEG10, PLEKHG4B, RND2, SV2A,* and *TUBB2B* — were associated with improved OS and PFS (Figure 5)

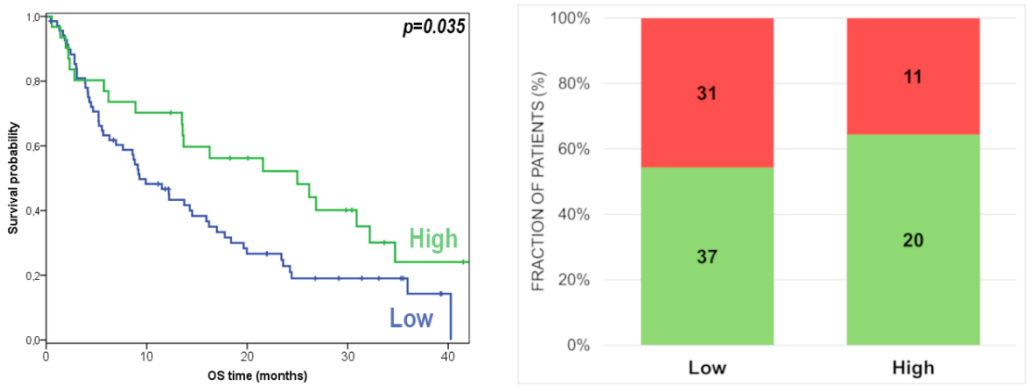

Figure 5. Survival and radiographic response of patients with low (<3.2) versus high (>3.2) neuronal signature score. Radiographic response is indicated as green for non-progressive disease (non-PD) and red for progressive disease (PD). (Own figure)

4.2.6. Combined model of clinicopathological and gene expression data

We used the Random Survival Forest model to identify the best prognostic model combining clinicopathological and molecular factors that showed significant associations with OS in univariate analysis. An additional inclusion criteria was the availability of the given parameter for at least 80% of the patients in order to avoid small sample sizes. We randomized our dataset into a training subcohort (75%) to develop the prediction algorithm and a test subcohort (25%), to evaluate the trained classifier. We calculated both the area under the receiver operating characteristic (ROC) curves (AUC) and the concordance index (C-index) for the developed predictions. Our final model included four laboratory parameters (LDH, Hg, eGFR, NLR) and 10 gene-expression based markers (*CR2, HLA-E, IRF7, PSMB10, PSMB8, CXCL12, IL12A, MAP2K4, IRF1*, Neuronal signature score). The AUC and the C-index of this prediction were 0.89 and 0.77 on the test set, respectively (Figure 6A-B). Each patient was assigned a score based on this prediction model, and using the median score (38.5), patients could be divided into low-

score and high-score groups. The median overall survival (OS) of the high-score group was inferior to that of the low-score group (7.6 months *vs.* 40.3 months, HR=10.86, p=0.002) (Figure 6C).

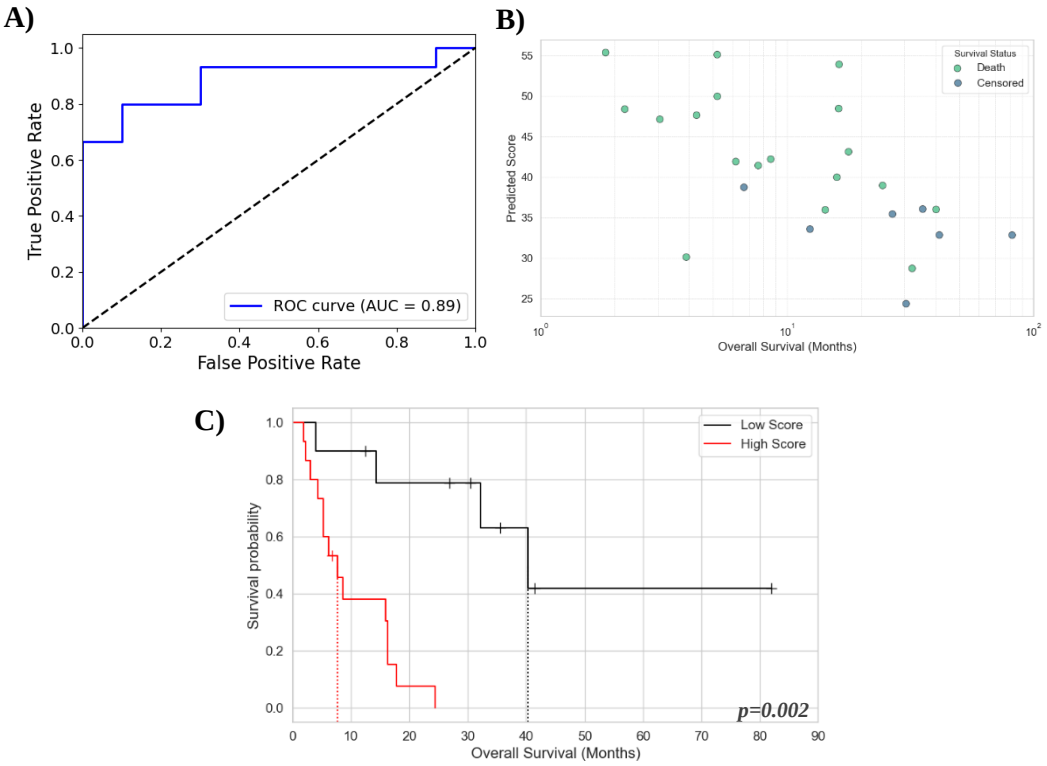

Figure 6. The best combination model's performance and survival analysis: ROC Curve (A), Survival *vs.* score scatter plot (B) and Kaplan-Meier plot (C). (Own figure)

4.3. Soluble PD-L1 concentration in serum samples

Serum samples before ICI initiation (baseline) were available from 10 male and 2 female UC patients. Only one patient was treated with pembrolizumab, all of the others received atezolizumab therapy. The median of the baseline sPD-L1 concentration was 90.0 pg/ml (range: 25.3-169.0). On-treatment serum samples, collected before the second immunotherapy cycle, were available for 11 patients with a median sPD-L1 concentration of 2316.0 pg/ml (range: 42.5-3818.6). Eight cycles (range: 2-47) was the median therapy lengths. The median follow-up was 39.7 months (range: 2.2-63.6) with seven patients died within this period.

Although the limited number of cases did not allow for a valid statistical analysis, higher pre-treatment serum PD-L1 concentrations were associated with poor OS in Kaplan-Meier analysis dichotomized at the median (p=0.069) (Figure 7A).

Interestingly, a >25-fold increase could be observed in sPD-L1 concentrations in all on-treatment samples after atezolizumab treatment (Figure 7B), whereas no such increase was showed in the samples of the pembrolizumab-treated patient. To rule out a possible interference between the therapeutic antibody, atezolizumab and the ELISA kit, we performed an ELISA analysis with atezolizumab solution, which showed no positive reaction in our ELISA assay. This suggests no interference between the therapeutic anti-PD-L1 antibody and the antibodies used in the ELISA.

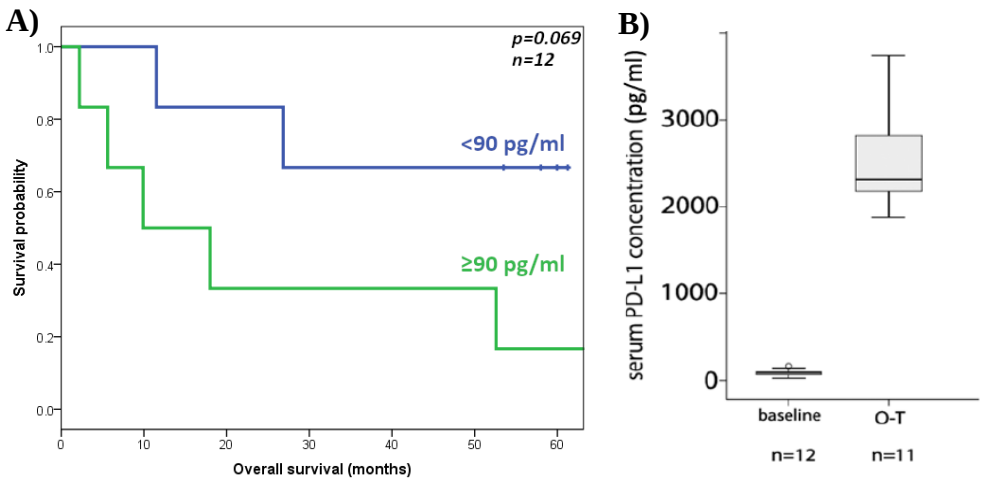

Figure 7. Overall survival stratified by pre-treatment sPD-L1 levels in ICI-treated patients (A) and box-plot presentation of serum PD-L1 levels in baseline and on-treatment (O-T) samples (collected at 2-3. therapy cycles (B).

5. Conclusion

This study investigated the efficacy of ICI therapy for UC in real-world clinical practice, finding atezolizumab and pembrolizumab effective for advanced or metastatic UC patients, regardless of treatment line, with second-line atezolizumab showing better outcomes than respective clinical trials. The study emphasized the need for easily accessible prognostic and predictive markers, such as clinicopathological and laboratory parameters, to optimize treatment decisions. Key prognostic factors included ECOG PS, metastasis sites, NLR, hemoglobin, albumin, and eGFR levels. The Bellmunt risk score's utility could be confirmed, and its performance could be further improved by adding CRP to the model. Our study provides valuable real-world insights, highlighting key similarities and differences compared to approval studies. These findings can inform larger meta-analyses and contribute to high-level clinical conclusions, helping to position ICI therapy within the complex treatment landscape of mUC.

In addition, we analyzed the expression of over 700 immune-related genes to identify potential ICI-predictive biomarkers in our institutional UC patient cohort. We found 23 genes with significant prognostic value and 43 genes significantly associated with DCR. Validation in a large, independent transcriptome dataset of ICI-treated UC patients confirmed the prognostic and predictive significance of *PSMB10*.

We used a novel gene-panel-based approach to classify the tumor tissue samples into molecular subtypes according to four various classification systems and assessed the predictive value of molecular subtype classification in the context of ICI therapy. We identified the highest ORR and OS in TCGA-luminal infiltrated, Lund-mesenchymal, and MDA p53-like subtypes. Although neuronal subtypes showed promising ICI responses, small case numbers limited statistical robustness. Analyzing neuronal signature scores revealed that high scores correlated with improved OS and PFS, suggesting that even non-neuronal subtypes with elevated neuronal signature scores may benefit from ICI therapy.

By combining different laboratory and gene expression based parameters, we developed a prognostic model, the applicability of which needs to be evaluated in other ICI-treated UC cohorts or within the framework of a prospective study, in order to help to optimize therapeutic decision-making in the future.

Finally, we evaluated the prognostic value of the serum biomarker sPD-L1 and found that higher pre-treatment serum PD-L1 levels are associated with poor OS in ICI-treated UC patients, although the small sample size limits the strength of this finding.

Our study identified a series of clinicopathological, laboratory, serum, and gene expression-based markers that could help to optimize the disease management of UC, pending validation in prospective clinical studies.

6. Bibliography of own publications

Publications related to the PhD thesis:

1. **Váradi M**, Horváth O, Módos O, Fazekas T, Grunewald CM, Niegisch G, Krafft U, Grünwald V, Hadaschik B, Olah C, Maráz A, Furka A, Szűcs M, Nyirády P, Szarvas T. Efficacy of immune checkpoint inhibitor therapy for advanced urothelial carcinoma in real-life clinical practice: results of a multicentric, retrospective study. Sci Rep. 2023;13(1):17378. **IF:3.8**

2. Krafft U, Olah C, Reis H, Kesch C, Darr C, Grünwald V, Tschirdewahn S, Hadaschik B, Horvath O, Kenessey I, Nyirady P, **Varadi M**, Modos O, Csizmarik A, Szarvas T. High Serum PD-L1 Levels Are Associated with Poor Survival in Urothelial Cancer Patients Treated with Chemotherapy and Immune Checkpoint Inhibitor Therapy. Cancers (Basel). 2021; 13: 2548. **IF:6.575**

3. Olah C, Hahnen C, Nagy N, Musial J, **Varadi M**, Nyiro G, Gyorffy B, Hadaschik B, Rawitzer J, Ting S, Sjödahl G, Hoffmann MJ, Reis H, Szarvas T. A quantitative polymerase chain reaction based method for molecular subtype classification of urinary bladder cancer-Stromal gene expressions show higher prognostic values than intrinsic tumor genes. Int J Cancer. 2022;150(5):856-867. **IF:6.4**

4. Széles Á, Kovács PT, Csizmarik A, **Váradi M**, Riesz P, Fazekas T, Váncsa S, Hegyi P, Oláh C, Tschirdewahn S, Darr C, Krafft U, Grünwald V, Hadaschik B, Horváth O, Nyirády P, Szarvas T. High Pretreatment Serum PD-L1 Levels Are Associated with Muscle Invasion and Shorter Survival in Upper Tract Urothelial Carcinoma. Biomedicines. 2022;10(10):2560. **IF:4.757**

5. Széles Á, Fazekas T, Váncsa S, **Váradi M**, Kovács PT, Krafft U, Grünwald V, Hadaschik B, Csizmarik A, Hegyi P, Váradi A, Nyirády P, Szarvas T. Pre-treatment soluble PD-L1 as a predictor of overall survival for immune checkpoint inhibitor therapy: a systematic review and meta-analysis. Cancers Immunol Immun. 2023;72(5), 1061–1073. **IF:4.6**

Publications not related to the PhD thesis:

6. Módos O, Bozsaki Á, Nagy C, Habina-Nagy N, Pásztor-Csizmarik A, Keresztes D, C. Oláh, **Váradi M**, Horváth A, Szendrői A, Szűcs M, Keszthelyi A, Nyirády P, Szarvas T. A platinaalapú kemoterápia szerepe a húgyhólyagrák kezelésében – az elmúlt 10 év klinikai tapasztalatainak feldolgozása. Magyar Urológia. 2019;31(2):58-65.

7. Nagy N, Kubik A, Szendrői A, Kenessey I, Módos O, Csizmarik A, **Váradi M**, Keresztes D, Szász MA, Hegyi L, Kovalszky I, Reis H, Hadaschik B, Nyirády P, Szarvas T. Combination of molecular genetic analysis with decision-supporting database in order to identify potentially effective drugs for rare adenocarcinomas of the urinary bladder. Orvosképzés. 2020;95(1):95-.

8. Szarvas T, Hoffmann MJ, Olah C, Szekely E, Kiss A, Hess J, Tschirdewahn S, Hadaschik B, Grotheer V, Nyirady P, Csizmarik A, **Varadi M**, Reis H. MMP-7 Serum and Tissue Levels Are Associated with Poor Survival in Platinum-Treated Bladder Cancer Patients. Diagnostics (Basel). 2020; 11: 48. **IF:3.992**

9. Szarvas T, Csizmarik A, Nagy N, Keresztes D, **Váradi M**, Küronya Z, Riesz P, Nyirády P. Az áttétes kasztrációrezisztens prosztatarák gyógyszer-rezisztenciájának molekuláris vonatkozásai. Orv Hetil. 2020; 161: 813-820. **IF:0.54**

10. Szarvas T, Csizmarik A, **Váradi M**, Fazekas T, Hüttl A, Nyirády P, Hadaschik B, Grünwald V, Tschirdewahn S, Shariat SF, Sevcenco S, Maj-Hes A, Kramer G. The prognostic value of serum MMP-7 levels in prostate cancer patients who received docetaxel, abiraterone, or enzalutamide therapy. Urol Oncol. 2021; 39: 296.e11-296.e19. **IF:2.954**

11. Oláh C, **Váradi M**, Kordáné Horváth O, Nyirády P, Szarvas T. A béltartalom és a vizelet mikrobiom-összetételének onkológiai vonatkozásai. Orv Hetil. 2021;162(15):579-86. **IF:0.707**

12. Szarvas T, Pásztor-Csizmarik A, **Váradi M**, Oláh C, Nyirády P. A prosztatarák és húgyhólyagrák molekuláris hátterének terápiás vonatkozásai. Orvosképzés. 2021;96(3):413-421.

13. Kovács PT, Mayer T, Csizmarik A, **Váradi M**, Oláh C, Széles Á, Tschirdewahn S, Krafft U, Hadaschik B, Nyirády P, Riesz P, Szarvas T. Elevated Pre-Treatment Serum MMP-7 Levels Are Associated with the Presence of Metastasis and Poor Survival in Upper Tract Urothelial Carcinoma. Biomedicines. 2022; 10: 698. **IF:4.757**

14. Kubik A, Pinto Amorim das Virgens I, Szabó A, **Váradi M**, Pásztor-Csizmarik A, Keszthelyi A, Majoros A, Fehérvári P, Hegyi P, Ács N, Nyirády P, SzarvasT.

Comprehensive Analysis of the Prognostic Value of Circulating MMP-7 Levels in Urothelial Carcinoma: A Combined Cohort Analysis, Systematic Review, and Meta-Analysis. Int J Mol Sci. 2023;24(9). **IF:4.9**

15. Módos O, **Váradi M**, Dér B, Keszthelyi A, Szűcs M, Reis H, Nyirády P, Szarvas T. Az urachuscarcinoma aktuális diagnosztikai és kezelési lehetőségei. Orv Hetil. 2023;164(16):602-609. **IF:0.8**

16. Olah C, Reis H, Hoffmann MJ, Mairinger F, Ting S, Hadaschik B, Krafft U, Grünwald V, Nyirady P, **Varadi M**, Győrffy B, Kiss A, Szekely E, Sjödahl G, Szarvas T. Predictive value of molecular subtypes and APOBEC3G for adjuvant chemotherapy in urothelial bladder cancer. Cancer Med. 2023;12:5222-5232. **IF:2.9**

17. **Varadi M**, Nagy N, Reis H, Hadaschik B, Niedworok C, Modos O, Szendroi A, Ablat J, Black PC, Keresztes D, Csizmarik A, Olah C, Gaisa NT, Kiss A, Timar J, Toth E, Csernak E, Gerstner A, Mittal V, Karkampouna S, Kruithof de Julio M, Gyorffy B, Bedics G, Rink M, Fisch M, Nyirady P, Szarvas T. Clinical sequencing identifies potential actionable alterations in a high rate of urachal and primary bladder adenocarcinomas. Cancer Med. 2023;12(7):9041-9054. **IF: 2.9**

18. Csizmarik A, Nagy N, Keresztes D, **Váradi M**, Bracht T, Sitek B, Witzke K, Puhr M, Tornyi I, Lázár J, Takács L, Kramer G, Sevcenco S, Maj-Hes A, Hadaschik B, Nyirády P, Szarvas T. Comparative proteome and serum analysis identified FSCN1 as a marker of abiraterone resistance in castration-resistant prostate cancer. Prostate Cancer Prostatic Disease. 2024;27:451-456. **IF: 5.1**

19. Oláh C, Shmorhun O, Klamminger G, Rawitzer J, Sichward L, Hadaschik B, Al-Nader M, Krafft U, Niedworok C, Váradi M, Nyirády P, Kiss A, Székely E, Reis H, Szarvas T. Immunohistochemistry-based molecular subtypes of urothelial carcinoma derive different survival benefit from platinum chemotherapy. Journal of Pathology: Clinical Research. 2025 Jan;11(1):e70017. **IF:3.4**

∑IF: 62.817